AIJR Preprints
Section: Coronavirus
Article Id: 158, Version: 1, 2020
URL: https://preprints.aijr.org/index.php/ap/preprint/view/158
{Click on above link to see the latest available version of this article}

NOT PEER-REVIEWED

Version 1: Received: 04 July 2020 / Approved: 08 July 2020 / Online: 08 July 2020

Deep Learning Classififcation For Diagnosis COVID-19 Between Bacterial Pneumonia and Viral Pneumonia in Chest X-Ray Images

Ahmed Abdullah Farid[1*], Gamal Ibrahim Selim[1], Hatem Awad A. Khater[2]

[1] Department of Computer Engineering, Faculty of Engineering & Technology, Arab Academy for Science Technology and Maritime Transport(AASTMT), Cairo, Egypt
[2] Faculty of Engineering, Horus University in Egypt

*Corresponding author (email:***************).

ABSTRACT

The novel coronavirus disease (COVID-19) was identified in the city of Wuhan, China at the end of 2019 as novel illness pneumonia. Today, it's being an epidemic around the world, the amount of sick people and fatalities increases growing increasingly every day according to the World Health Organisation (WHO) revised statistics. The purpose of this article is therefore to incorporate a new deep learning Images Classifiers, to diagnose COVID-19 and differentiate it between (Normal, Bacterial Pneumonia, Viral Pneumonia) in X-ray Images. The study is validated on 2002 Chest X-ray images with 60 confirmed positive COVID-19 cases and (650 x-rays bacterial pneumonia, 412 x-ray viral pneumonia, 880 normal x-rays) images. The proposed architectures of the deep convolutional neural network model (DCNN-COVID-NET) can analyze the normalized intensities of the X-ray image to classify the patient status as (normal,bacterial , viral , COVID-19) pneumonia case, In comparison with (VGG19) and (DenseNet, ResNetV2, InceptionV3, InceptionResNetV2, Xception, MobileNetV2) of deep convolutional neural network models. Experiments and evaluation of the proposed (DCNN-COVID-NET) have been successfully done based on 80-20% of Xray images for the model training and testing phases, respectively. The (DCNN-COVID-NET) Convolutional Network model showed a good performance of automated COVID-19 classification with f1-scores of 1.00 and 0.98 for normal and COVID-19, respectively among other deep convolutional neural network models. This study demonstrated the useful deep learning model to classify COVID-19 in chest X-ray images based on the proposed (DCNN-COVID-NET).

Keywords: Bacterial -Viral *Pneumonia, COVID-19, X-ray Image, Deep Learning,* Convolution Neural Network

1. Introduction

Coronaviruses (Covid-19) are a wide family of dangerous viruses [1]. The Covid-19 is so-called because of its distinctive solar corona (crown-like) presence when viewed under an electron microscope [2]. They can cause serious and infectious diseases such as Extreme Acute Respiratory Syndrome (SARS-CoV) and Respiratory

How to Cite:

Ahmed Abdullah Farid *et al.* "Deep Learning Classififcation For Diagnosis COVID-19 Between Bacterial Pneumonia and Viral Pneumonia in Chest X-Ray Images". *AIJR Preprints*, 158, version 1, 2020. https://preprints.aijr.org/index.php/ap/preprint/view/158

Syndrome of the Middle East (MERS-CoV). After December 2019[3-6] the outbreak of the 2019 novel coronavirus in Wuhan, China has been spreading rapidly to other countries of the world. The World Health Organisation (WHO) on 11 February 2020 identified the infectious disease triggered by these viruses as COVID-19[7].There have been 82,758 confirmed cases to China to date (April 22, 2020), and 2,552,157 confirmed cases worldwide [8], and 177,230 confirmed death cases worldwide [45][47].

While the sputum's real-time polymerase chain reaction (RT-PCR) assay is the gold standard for the diagnosis of Coronaviruses, testing COVID-19 patients is time-consuming due to the large false-negative levels[9]. Medical imaging methodologies such as chest X-ray (CXR) and computed tomography (CT) may thus play a major role in confirming positive COVID-19 patients, especially in cases of infected pregnant women and children[10, 11]. Previous research to classify COVID-19 also studied volumetric CT thorax pictures for the lung and soft tissue[10, 12]. The key downside to utilizing CT visualization, however, is the heavy dosage to patients and the expense scan[13][48]. Conversely, traditional radiographic or CXR devices are required in both hospitals and clinics for the creation of 2-dimensional (2D) thorax projection images. The CXR modality is typically the first option for radiologists to diagnose chest pathology and was used to classify or validate COVID-19 in a limited number of patients[10, 14][49]. The emphasis of this research is therefore only on the usage of the X-ray imaging modality for possible COVID-19 patients.

However, X-ray images cannot readily discern soft tissue with a weak contrast to reduce the patients' exposure dose [13, 15]. Computer-aided diagnostic (CAD) programs have been developed to enable doctors accurately identify and measure presumed diseases in critical organs in X-ray images[16, 17][50] to resolve these limitations. CAD systems rely primarily on the rapid advancement of digital technologies such as graphics processing units (GPUs) to operate algorithms for medical image processing, including model enhancement, organ and/or tumor segmentation, and interventional navigation tasks[18-20]. Today, in many medical fields, artificial intelligence technologies such as machine learning and deep learning are the cornerstone of sophisticated CAD systems; for example, respiratory diseases[21, 22], cardiology[23, 24], and brain surgery[25, 26][46-50].

Deep learning mechanisms have demonstrated positive results in the last few years in performing radiological tasks by automatically decoding multimodal medical images[27-29]. Deep convolutionary neural networks (DCNNs) are one of the efficient architectures in deep learning, which have been commonly implemented intuitively in many functional applications such as pattern recognition which image classification[30]. DCNNs can manage neural network weight testing on very wide datasets[31][48-49], fine-tuning the network weights of a pre-trained DCNN based on limited datasets, applying unattended pre-training to determine network weights before implementing DCNN models in a system, The use of pre-trained DCNN is often referred to as off-the-shelf CNN that is used as an extractor feature[46-50].

In previous research, DCNNs were used to successfully identify specific chest diseases such as Tuberculosis screening[32] and mediastinal lymph nodes in CT images[33] in the X-ray image classification process. Nevertheless, the usage of deep learning methods in X-ray to classify and diagnose novel COVID-19 is still very minimal up to now. The goal of this study is therefore to introduce a new model for pre-trained deep learning classifiers; namely (DCNN-COVID-NET) as an advanced method to support radiologists diagnose COVID-19 automatically in X-ray images to automatically assist the early diagnosis of patients with COVID-19 efficiently[49].

Also, an analytical review of the proposed deep learning image classifiers is carried out in the role of classifying COVID-19 disease utilizing traditional chest X-rays at a lower expense than other imaging modalities such as CT. Reporting the comparative output of various deep learning models with remarks showing the most reliable classification results of COVID-19 using a limited X-ray image dataset[49].

The rest of this paper is structured as follows. Section 2 gives a review on the state-of-the-art deep convolutional neural network models as image classifiers. Also, a detailed description of the (DCNN-COVID-NET) is presented. Experimental results and comparative performance of the proposed deep learning classifiers are investigated and discussed in section 3. Finally, this study is concluded with the main prospects in section 4.

2. Methods

2.1 Deep learning image classifiers

In this section, we describe some of the existing state-of-the-art deep learning image classifiers that are required to accomplish the clinical purpose of the (DCNN-COVID-NET) framework as follows.

i ***VGG19*:** The Visual Geometry Group Network (VGG) was developed on the basis of the convoluted neural network architecture of Karen Simonyan and Andrew Zisserman, Oxford Robotics Institute[34]. It was addressed at the 2014 Large Scale Visual Recognition Challenge (ILSVRC2014). The VGGNet performed very well on the imageNet dataset. In order to have improved image extraction functionality, the VGGNet used smaller filters of 3×3, compared to AlexNet 11×11 filter[49]. There are two versions of this deep network architecture; namely VGG16 and VGG19 have different depths and layers. VGG19 is deeper than VGG16.The number of parameters for VGG19, however, is larger and thus more expensive than VGG16 to train the network[46-50].

ii ***DenseNet121:*** The Dense Convolutional Network (DenseNet) have several compelling benefits: they lighten the vanishing-gradient problem, reinforce feature propagation, encourage feature reuse, and the number of parameters reduced substantially [35][46]. DenseNet121 is a Dense Net model which generated with 121 layers, the model was loaded with pre-trained weights from ImageNet database[46-50].

iii ***InceptionV3:*** Inception network or GoogLeNet was 22-layer network and it won 2014 Image net challenge with 93.3% top-5 accuracy [36]. "Later versions are referred as Inception VN where N is the version number so inceptionV1, inceptionV2and inceptionV3. The Inception V3 network has several symmetrical and asymmetrical building blocks, where each block has several branches of convolutions, average pooling, maxpooling, concatenated, dropouts, and fully-connected layers"[46-50].

iv ***ResNetV2:*** He *et al.* [37] developed the Residual Neural Network (ResNet) models by utilizing skip connections to jump over some network layers to achieve strong convergence behaviors. The improved version of ResNet is called ResNet-V2. Although the ResNet is similar to the VGGNet, it is approximately eight times deeper [38][46-50].

v ***Inception-ResNet-V2:*** A convolutional neural network is 164 layers deep, combining the Inception architecture with residual connections. Inception-ResNet-V2 is a variation of InceptionV3 [47-50]. InceptionResNet-V2 is trained on more than a million images from the ImageNet database.

vi ***Xception:*** The architecture of Xception model is a linear stack of depth wise separable convolution layers with residual connections to easily define and modify the deep network architecture [40]. "The Xception is an enhancement of the Inception architecture that replaces regular inception modules with distinguishable depth convolutions"[46-50]**.**

vii ***MobileNetV2:*** Sandler *et al*. [41-47] proposed the MobileNetV2 model as a convolutional neural network architecture for machines with limited computing power, like smartphones." The MobileNets achieve this key advantage by reducing the number of learning parameters, and introducing the inverted-residuals-with-linearbottleneck-blocks to greatly reduce the memory consumption. Moreover, the pre-trained implementation of Mobile NetV2 is widely available in many popular deep learning frameworks"[46-50].

2.2 Proposed (DCNN-COVID-NET) Description

We proposed a new deep learning framework for automatically identifying the status of COVID-19 in 2D conventional chest X-ray images. Fig. 1 ,Fig. 2 ,Fig. 3 depicts the overall workflow of our proposed (DCNN-COVID-NET) based on 2 convolution neural network 20 filter and 50 filter[49].

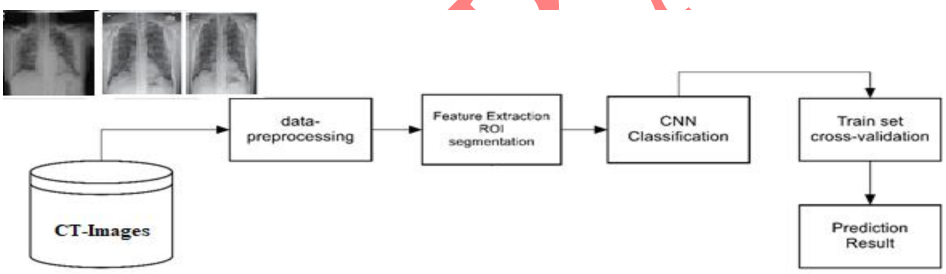

Fig 1. The Framework structure

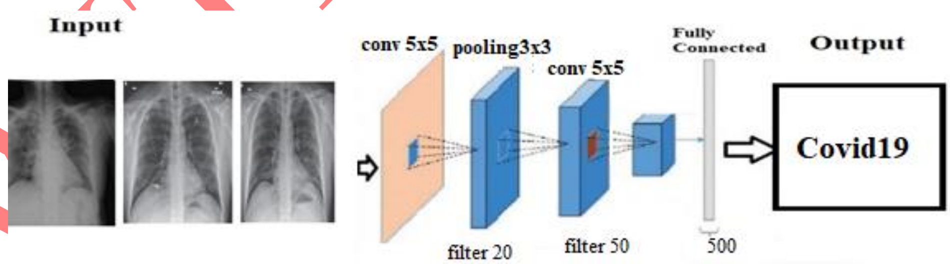

Fig 2. The CNN Network Structure

Fig 3. Architecture of CNN Model

The (DCNN-COVID-NET) framework includes three main steps to accomplish the diagnostic procedure of novel Coronavirus, as follows.

- **Preprocessing**

All X-ray images were collected in one data set and loaded for scaling at a fixed size of 224 X 224 pixels to be suitable for further processing in the deep learning pipeline. One-hot encoding[42] is then applied to the image data labels to indicate the positive case of COVID-19 or "not" for each image in the dataset[49].

- **Training Model and Validation**

In order to start the training step of one of the seven deep learning models chosen and/or modified, the pre-processed data set is 80-20 divided according to the Pareto principle. It means that 20% of the picture data would be required for the processing process. Again, separating 80 percent data would be used to create equivalent training and validation sets. Sub-sample random collections of training image data for the deep learning classifier, and then add assessment metrics to display the reported output of the validation package[49].

- **Classification**

In the final stage of the proposed system, the test data is fed to the tuned deep learning classifier to categorize all picture patches in one of two cases: verified positive COVID-19 or regular case (negative COVID-19) as shown in Fig. 1. At the conclusion of the process, the cumulative output review of each deep learning classifier will be analyzed based on the parameters mentioned in the following section[46-50].

2.3 Classification Performance Analysis

In order to test the output of each deep learning model in the (DCNN-COVID-NET) sample, various parameters have been used in this analysis to calculate the accurate and/or incorrect classification of the COVID-19 identified in the Xray images as follows. First, the cross validity estimator [43-47] was used and resulted in a uncertainty matrix as seen in Fig.4. The uncertainty equation has as follows four predicted outcomes. True Positive (TP) is a collection of abnormalities that have been reported with the proper diagnosis. Real Negative (TN) is a number of daily instances wrongly counted. False Positive (FP) is a collection of regular cases classified as FP anomaly diagnoses.

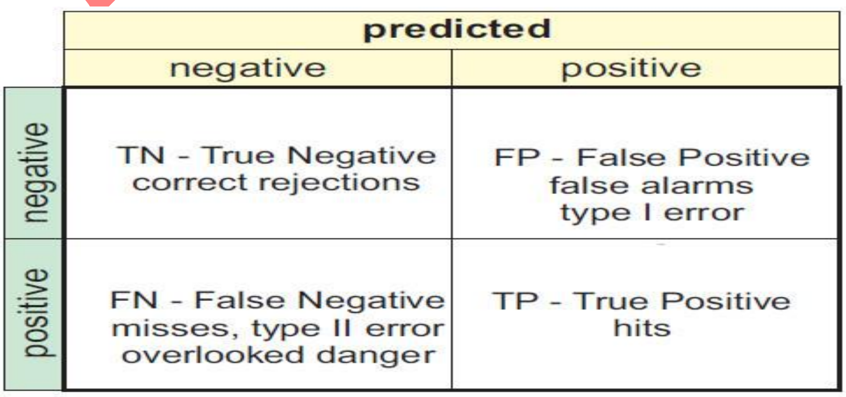

Fig.4. Confusion Matrix

After calculating the values of possible outcomes in the confusion matrix, the following performance metrics can be calculated.

A) Accuracy: Accuracy is the most significant metric for the performance of our deep learning classifiers, as described out in (1). This is essentially a percentage of the true positive and true negatives separated by the combined values of the uncertainty matrix elements. The most accurate model is the optimal one, but it is important to insure that there are symmetric datasets with nearly equivalent false positive values and false adverse values. The above components of the uncertainty matrix must therefore be determined in order to determine the classification efficiency of our proposed (DCNN-COVID-NET) framework[46].

$$\text{Accuracy}(\%)=\frac{TP+TN}{TP+FP+FN+TN}100\% \qquad (1)$$

B) Precision: Precision is represented in (2) to give relationship between the true positive predicted values and full positive predicted values[47].

$$\text{Precision}=\frac{TP}{TP+FP} \qquad (2)$$

C) Recall: In (3), recall or sensitivity is the ratio between the true positive values of prediction and the summation of predicted true positive values and predicted false negative values[48].

$$\text{Recall}=\frac{TP}{TP+FN} \qquad (3)$$

D) F1-score: F1-score is an overall measure of the model's accuracy that combines precision and recall, as represented in (4). F1-score is the twice of the ratio between the multiplication to the summation of precision and recall metrics[49].

$$\text{F1-score}=2\left(\frac{\text{Precision Recall}^{\square}}{\text{Precision+Recall}}\right) \qquad (4)$$

3 Experiments

3.1 Dataset and Experimental setup

The dataset of chest X-ray images used in this study for classifying negative and positive COVID-19 cases from bacterial pneumonia and viral pneumonia. The dataset includes 2002 X-ray images, divided into four classes as with 60 confirmed positive COVID-19 cases and (650 x-rays bacterial pneumonia, 412 x-ray viral pneumonia, 880 normal x-rays) images. Fig. 5 shows a sample of normal and COVID-19 images extracted from the dataset. The X-ray images for confirmed COVID-19 disease show a pattern of ground-glass opacification with occasional consolidation in the patchy, peripheral, and bilateral areas [10]. The original size of tested images is 400x300 pixels. For the experimental setup, all images were scaled to the size of 227 × 227 pixels. The (DCNN-COVID-NET) framework including deep learning classifiers have been implemented using Weka [44] on Intel(R) Core(TM) i7-2.2 GHz processor. In addition, the experiments were executed using the graphical processing unit (GPU) NVIDIA GTX 1050 Ti and RAM with 4 GB and 16 GB, respectively.

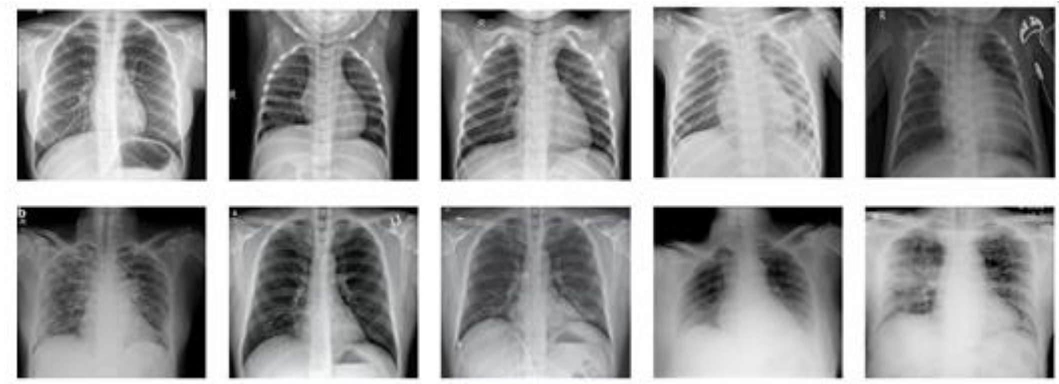

Fig 5. A sample of X-ray images

3.2 Overall Performance Evaluation

To order to test the efficiency of potential deep learning classifiers, 80 % of X-ray pictures, both regular and diseased instances, are randomly chosen for processing, i.e. 40 pictures of the dataset. The training parameters for all DCNN architectures in this analysis are: the learning rate = e−3, the values of the batch size and the number of epochs are set to 7 and 50, respectively, to achieve the optimal convergence with few iterations on this chest X-ray image dataset, and also to prevent the issue of degradation as possible. Both deep network classifiers are trained using Stochastic Gradient Descent (SGD) because of their strong converging and quick running time.

Table 2 illustrates the comparative computational times and the accuracy of tested deep learning image classifiers. The running times of all deep learning models are relatively short ranging from 390.0 to 2645.0 seconds because of using powerful capabilities of the GPU with a chest X-ray image dataset. The resulting test times of the (DCNN-COVID-NET) models did not exceed 6 seconds on the 20 images examined, as shown in Fig. 3. Among all the tested classifiers, the accuracy of the InceptionV3 model was the worst of 50 %, while the VGG19 and DenseNet201 models achieved the best accuracy (90 %). While the MobileNetV2 model showed a modest accuracy value (60 %), it achieved the smallest computational times of 389.0 and 1.0 seconds for training and testing phases, respectively, as listed in Table. 1. In addition, the values of performance metrics of each deep learning classifier are presented in Table 2. The highest precision of deep learning classifier to detect only positive COVID-19 was achieved by ResNetV2, InceptionResNetV2, Xception, and MobileNetV2, but their corresponding performances were worst to classify the normal cases correctly. **Therefore, we compare our porposed CNN deep learning of two convolution newtwork {20,50} filters with this traditional and got 98.20% accuracy.**

In comparison, Fig. 3 displays the graphical output assessment of all qualified deep learning classifiers with accuracy and cross-entropy loss (loss) during the training and validation process. The highest training scores and testing performance were obtained for the VGG19 and DenseNet201 versions, and the worst case is the InceptionV3, as seen in Table 3. The corresponding uncertainty matrices of all the deep learning classifiers evaluated are seen in Fig. 4. In addition, our findings have applied the Receiver Operational Characteristics (ROC) curves to validate the classification efficiency of. deep learning classifier by displaying the true positive rate (TPR) against the false positive rate (FPR) to identify the positive COVID-19 cases in the tested X-ray images.

Table 1: Computational times and classification accuracy of all tested deep learning models of the (DCNN-COVID-NET) on a GPU.

Classifier	Training Time (seconds)	Testing Time (seconds)	Accuracy (%)
VGG19	2641.00	4.00	90
DenseNet201	2122.00	6.00	90
ResNetV2	1086.00	2.00	70
InceptionV3	1121.00	2.00	50
InceptionResNetV2	1988.00	6.00	80
Xception	2035.00	3.00	80
MobileNetV2	389.00	1.00	60

Table 2: Comparative classification performance of deep learning models used in the (DCNN-COVID-NET)

Classifier	Patient Status	Precision	Recall	F1-score
VGG19	***COVID-19***	0.83	1.00	0.91
	Normal	1.00	0.80	0.89
DenseNet201	***COVID-19***	0.83	1.00	0.91
	Normal	1.00	8.00	0.89
ResNetV2	***COVID-19***	1.00	0.40	0.57
	Normal	0.62	1.00	0.77
InceptionV3	***COVID-19***	0.00	0.00	0.00
	Normal	0.50	1.00	0.67
InceptionResNetV2	***COVID-19***	1.00	0.60	0.75
	Normal	0.71	1.00	0.83
Xception	***COVID-19***	1.00	0.60	0.75
	Normal	0.71	1.00	0.83
MobileNetV2	***COVID-19***	1.00	0.20	0.33
	Normal	0.56	1.00	0.71

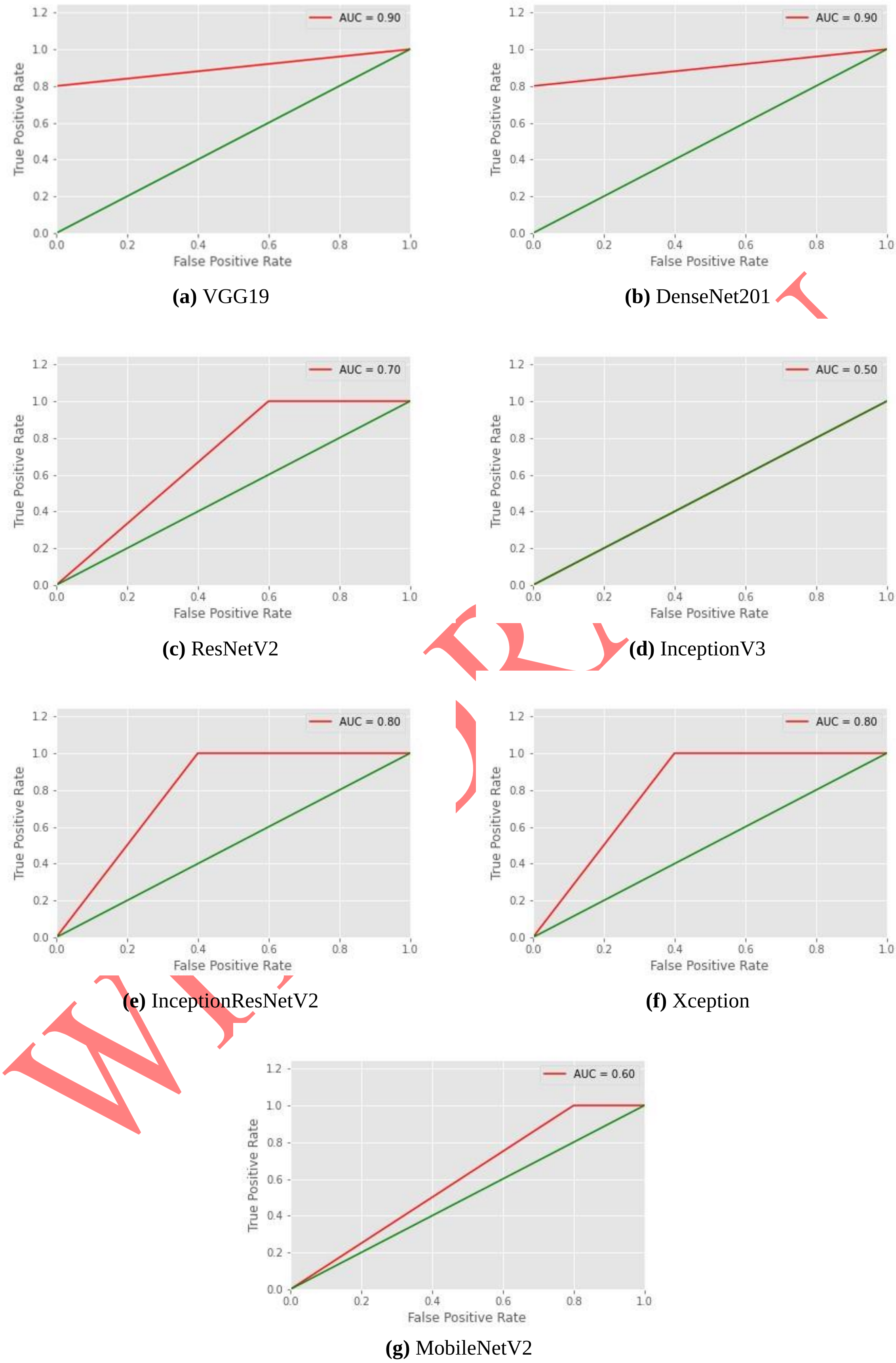

Fig 6 ROC curves of all deep learning models in the (DCNN-COVID-NET)

```
=== Classifier model  ===

Network Configuration:
NeuralNetConfiguration(weightInit=XAVIER, biasInit=0.0, dist=weka.dl4j.distribution.Disabled@66, l1=NaN, l2=NaN, dropout=Dropout(),
Model Summary:

================================================================================================
VertexName (VertexType)        nIn,nOut     TotalParams   ParamsShape                 Vertex Inputs
================================================================================================
input (InputVertex)            -,-          -             -                           -
cnn1 (ConvolutionLayer)        1,20         520           W:{20,1,5,5}, b:{1,20}      [input]
maxpool1 (SubsamplingLayer)    -,-          0             -                           [cnn1]
cnn2 (ConvolutionLayer)        20,50        25,050        W:{50,20,5,5}, b:{1,50}     [maxpool1]
maxpool2 (SubsamplingLayer)    -,-          0             -                           [cnn2]
ffn1 (DenseLayer)              72200,500    36,100,500    W:{72200,500}, b:{1,500}    [maxpool2]
output (OutputLayer)           500,4        2,004         W:{500,4}, b:{1,4}          [ffn1]
------------------------------------------------------------------------------------------------
            Total Parameters:  36,128,074
        Trainable Parameters:  36,128,074
           Frozen Parameters:  0
================================================================================================


Time taken to build model: 8900.94 seconds

=== Evaluation on training set ===

Time taken to test model on training data: 34.88 seconds

=== Summary ===

Correctly Classified Instances        1966               98.2018 %
Incorrectly Classified Instances        36                1.7982 %
Kappa statistic                          0.9726
Mean absolute error                      0.0111
Root mean squared error                  0.0826
Relative absolute error                  3.3852 %
Root relative squared error             20.3626 %
Total Number of Instances             2002

=== Detailed Accuracy By Class ===

                 TP Rate  FP Rate  Precision  Recall   F-Measure  MCC      ROC Area  PRC Area  Class
                 0.995    0.024    0.953      0.995    0.974      0.961    0.998     0.994     BacterialPneumonia
                 1.000    0.000    1.000      1.000    1.000      1.000    1.000     1.000     COVID
                 1.000    0.001    0.999      1.000    0.999      0.999    1.000     1.000     Normal
                 0.920    0.002    0.992      0.920    0.955      0.945    0.997     0.993     ViralPneumonia
Weighted Avg.    0.982    0.008    0.983      0.982    0.982      0.976    0.999     0.997

=== Confusion Matrix ===

   a   b   c   d   <-- classified as
 647   0   0   3 |   a = BacterialPneumonia
   0  60   0   0 |   b = COVID
   0   0 880   0 |   c = Normal
  32   0   1 379 |   d = ViralPneumonia
```

Fig 7. Confusion matrix of our proposed CNN classification model

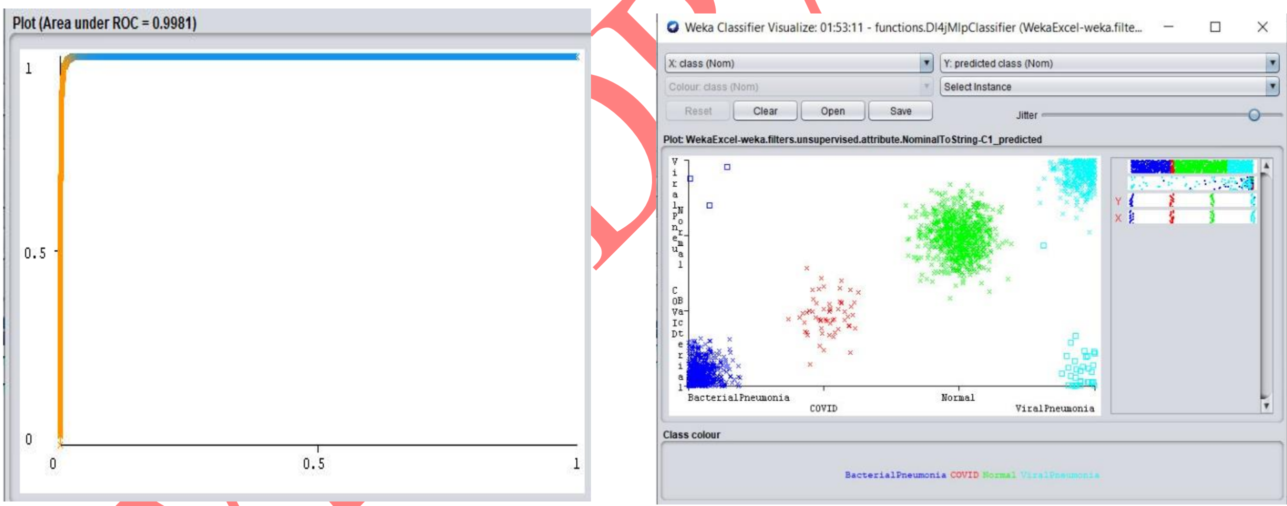

Fig 8. Roc with error curve for proposed CNN classification model

Table3: The details of result from CNN-Model

F-measure	TPR	ROC	PRC
98.2%	98.2%	99.9%	99.7%

4 Conclusions

Infectious COVID-19 disease is still threating the lives of billions of people. In this study, a Novel CNN framework has been proposed to automatically identify or confirm COVID-19 in 2-D X-ray images compared with seven deep learning classifiers; namely VGG19, DenseNet121, ResNetV2, InceptionV3, InceptionResNetV2, Xception, and MobileNetV2. The results of our proposed (DCNN-COVID-NET) verified the best performance scores of deep learning classifiers of 98.20% accuracy and shows better than the traditional classification approaches and last state of the art result .

References

[1] C. I. Paules, H. D. Marston, and A. S. Fauci, "Coronavirus Infections—More Than Just the Common Cold," *JAMA*, vol. 323, no. 8, pp. 707-708, 2020.

[2] Y. Chen, Q. Liu, and D. Guo, "Emerging coronaviruses: Genome structure, replication, and pathogenesis," *Journal of Medical Virology*, vol. 92, no. 4, pp. 418-423, 2020.

[3] N. Zhu *et al.*, "A Novel Coronavirus from Patients with Pneumonia in China, 2019," *New England Journal of Medicine*, vol. 382, no. 8, pp. 727-733, 2020.

[4] Q. Li *et al.*, "Early Transmission Dynamics in Wuhan, China, of Novel Coronavirus–Infected Pneumonia," *New England Journal of Medicine*, 2020.

[5] J. Cohen and D. Normile, "New SARS-like virus in China triggers alarm," *Science*, vol. 367, no. 6475, pp. 234-235, 2020.

[6] T. Lupia, S. Scabini, S. Mornese Pinna, G. Di Perri, F. G. De Rosa, and S. Corcione, "2019 novel coronavirus (2019-nCoV) outbreak: A new challenge," *Journal of Global Antimicrobial Resistance*, vol. 21, pp. 22-27, 2020/06/01/ 2020.

[7] C. Sohrabi *et al.*, "World Health Organization declares global emergency: A review of the 2019 novel coronavirus (COVID-19)," *International Journal of Surgery*, vol. 76, pp. 71-76, 2020/04/01/ 2020.

[8] https://www.who.int/emergencies/diseases/novel-coronavirus-2019/media-resources/press-briefings.

[9] P. Huang *et al.*, "Use of Chest CT in Combination with Negative RT-PCR Assay for the 2019 Novel Coronavirus but High Clinical Suspicion," *Radiology*, vol. 295, no. 1, pp. 22-23, 2020.

[10] M.-Y. Ng *et al.*, "Imaging Profile of the COVID-19 Infection: Radiologic Findings and Literature Review," *Radiology: Cardiothoracic Imaging*, vol. 2, no. 1, p. e200034, 2020.

[11] H. Liu, F. Liu, J. Li, T. Zhang, D. Wang, and W. Lan, "Clinical and CT imaging features of the COVID19 pneumonia: Focus on pregnant women and children," *Journal of Infection*, 2020/03/21/ 2020.

[12] M. Chung *et al.*, "CT Imaging Features of 2019 Novel Coronavirus (2019-nCoV)," *Radiology*, vol. 295, no. 1, pp. 202-207, 2020.

[13] L. J. M. Kroft, L. van der Velden, I. H. Girón, J. J. H. Roelofs, A. de Roos, and J. Geleijns, "Added Value of Ultra–low-dose Computed Tomography, Dose Equivalent to Chest X-Ray Radiography, for Diagnosing Chest Pathology," *Journal of Thoracic Imaging*, vol. 34, no. 3, pp. 179-186, 2019.

[14] N. Chen *et al.*, "Epidemiological and clinical characteristics of 99 cases of 2019 novel coronavirus pneumonia in Wuhan, China: a descriptive study," *Lancet*, vol. 395, no. 10223, pp. 507-513, Feb 15 2020.

[15] M. E. Karar, D. R. Merk, V. Falk, and O. Burgert, "A simple and accurate method for computer-aided transapical aortic valve replacement," *Computerized Medical Imaging and Graphics*, vol. 50, pp. 31-41, 2016.

[16] D. R. Merk *et al.*, "Image-guided transapical aortic valve implantation: sensorless tracking of stenotic valve landmarks in live fluoroscopic images," (in eng), *Innovations*, vol. 6, no. 4, pp. 231-6, Jul 2011.

[17] M. Messerli *et al.*, "Computer-aided detection (CAD) of solid pulmonary nodules in chest x-ray equivalent ultralow dose chest CT - first in-vivo results at dose levels of 0.13mSv," *European Journal of Radiology*, vol. 85, no. 12, pp. 2217-2224, 2016/12/01/ 2016.

[18] X. Tian *et al.*, "Medical imaging and diagnosis of subpatellar vertebrae based on improved Laplacian image enhancement algorithm," *Computer Methods and Programs in Biomedicine*, vol. 187, p. 105082, 2020/04/01/ 2020.

[19] T. He, J. Hu, Y. Song, J. Guo, and Z. Yi, "Multi-task learning for the segmentation of organs at risk with label dependence," *Medical Image Analysis*, vol. 61, p. 101666, 2020/04/01/ 2020.

[20] R. Hannan, M. Free, V. Arora, R. Harle, and P. Harvie, "Accuracy of computer navigation in total knee arthroplasty: A prospective computed tomography-based study," *Medical Engineering & Physics*, 2020/03/04/ 2020.

[21] C. H. Liang, Y. C. Liu, M. T. Wu, F. Garcia-Castro, A. Alberich-Bayarri, and F. Z. Wu, "Identifying pulmonary nodules or masses on chest radiography using deep learning: external validation and strategies to improve clinical practice," *Clinical Radiology*, vol. 75, no. 1, pp. 38-45, 2020/01/01/ 2020.

[22] S. Hussein, P. Kandel, C. W. Bolan, M. B. Wallace, and U. Bagci, "Lung and Pancreatic Tumor Characterization in the Deep Learning Era: Novel Supervised and Unsupervised Learning Approaches," *IEEE Transactions on Medical Imaging*, vol. 38, no. 8, pp. 1777-1787, 2019.

[23] M. E. Karar, S. H. El-Khafif, and M. A. El-Brawany, "Automated Diagnosis of Heart Sounds Using Rule-Based Classification Tree," *Journal of Medical Systems,* journal article vol. 41, no. 4, p. 60, March 01 2017.

[24] M. E. Karar, D. R. Merk, C. Chalopin, T. Walther, V. Falk, and O. Burgert, "Aortic valve prosthesis tracking for transapical aortic valve implantation," (in Eng), *Int J Comput Assist Radiol Surg,* vol. 6, no. 5, pp. 583-590, Sep 16 2011.

[25] N. Ghassemi, A. Shoeibi, and M. Rouhani, "Deep neural network with generative adversarial networks pre-training for brain tumor classification based on MR images," *Biomedical Signal Processing and Control,* vol. 57, p. 101678, 2020/03/01/ 2020.

[26] H. Rathore, A. K. Al-Ali, A. Mohamed, X. Du, and M. Guizani, "A Novel Deep Learning Strategy for Classifying Different Attack Patterns for Deep Brain Implants," *IEEE Access,* vol. 7, pp. 24154-24164, 2019.

[27] L. Chen, P. Bentley, K. Mori, K. Misawa, M. Fujiwara, and D. Rueckert, "Self-supervised learning for medical image analysis using image context restoration," *Medical Image Analysis,* vol. 58, p. 101539, 2019/12/01/ 2019.

[28] F. Gao, H. Yoon, T. Wu, and X. Chu, "A feature transfer enabled multi-task deep learning model on medical imaging," *Expert Systems with Applications,* vol. 143, p. 112957, 2020/04/01/ 2020.

[29] M. Kim, C. Yan, D. Yang, Q. Wang, J. Ma, and G. Wu, "Chapter Eight - Deep learning in biomedical image analysis," in *Biomedical Information Technology (Second Edition)*, D. D. Feng, Ed.: Academic Press, 2020, pp. 239-263.

[30] D.-X. Zhou, "Theory of deep convolutional neural networks: Downsampling," *Neural Networks,* vol. 124, pp. 319-327, 2020/04/01/ 2020.

[31] T. K. K. Ho, J. Gwak, O. Prakash, J.-I. Song, and C. M. Park, "Utilizing Pretrained Deep Learning Models for Automated Pulmonary Tuberculosis Detection Using Chest Radiography," in *Intelligent Information and Database Systems*, Cham, 2019, pp. 395-403: Springer International Publishing.

[32] F. Pasa, V. Golkov, F. Pfeiffer, D. Cremers, and D. Pfeiffer, "Efficient Deep Network Architectures for Fast Chest X-Ray Tuberculosis Screening and Visualization," *Scientific Reports,* vol. 9, no. 1, p. 6268, 2019/04/18 2019.

[33] Y. Miki *et al.*, "Classification of teeth in cone-beam CT using deep convolutional neural network," *Computers in Biology and Medicine,* vol. 80, pp. 24-29, 2017/01/01/ 2017.

[34] K. Simonyan and A. Zisserman, "Very Deep Convolutional Networks for Large-Scale Image Recognition," 2014.

[35] G. Huang, Z. Liu, L. Van Der Maaten, and K. Q. Weinberger, "Densely connected convolutional networks," in *Proceedings - 30th IEEE Conference on Computer Vision and Pattern Recognition, CVPR 2017* vol. 2017-January, ed: Institute of Electrical and Electronics Engineers Inc., 2017, pp. 2261-2269.

[36] C. Szegedy, V. Vanhoucke, S. Ioffe, J. Shlens, and Z. Wojna, "Rethinking the Inception Architecture for Computer Vision," in *2016 IEEE Conference on Computer Vision and Pattern Recognition (CVPR)*, 2016, pp. 2818-2826.

[37] K. He, X. Zhang, S. Ren, and J. Sun, "Deep residual learning for image recognition," *Proceedings of the IEEE Computer Society Conference on Computer Vision and Pattern Recognition*, vol. 2016-Decem, pp. 770-778, 2016.

[38] E. C. Too, L. Yujian, S. Njuki, and L. Yingchun, "A comparative study of fine-tuning deep learning models for plant disease identification," *Computers and Electronics in Agriculture,* vol. 161, pp. 272279, 2019/06/01/ 2019.

[39] C. Szegedy, S. Ioffe, V. Vanhoucke, and A. A. Alemi, "Inception-v4, inception-ResNet and the impact of residual connections on learning," presented at the Proceedings of the Thirty-First AAAI Conference on Artificial Intelligence, San Francisco, California, USA, 2017.

[40] F. Chollet, "Xception: Deep learning with depthwise separable convolutions," in *Proceedings - 30th IEEE Conference on Computer Vision and Pattern Recognition, CVPR 2017* vol. 2017-January, ed: Institute of Electrical and Electronics Engineers Inc., 2017, pp. 1800-1807.

[41] M. Sandler, A. Howard, M. Zhu, A. Zhmoginov, and L. C. Chen, "MobileNetV2: Inverted Residuals and Linear Bottlenecks," *Proceedings of the IEEE Computer Society Conference on Computer Vision and Pattern Recognition,* pp. 4510-4520, 2018.

[42] S. L. Harris and D. M. Harris, "3 - Sequential Logic Design," in *Digital Design and Computer Architecture*, S. L. Harris and D. M. Harris, Eds. Boston: Morgan Kaufmann, 2016, pp. 108-171.

[43] M. Sokolova and G. Lapalme, "A systematic analysis of performance measures for classification tasks," *Information Processing & Management*, vol. 45, no. 4, pp. 427-437, 2009/07/01/ 2009.

[44] A. Gulli, A. Kapoor, and S. Pal, Deep Learning with TensorFlow 2 and Keras: Regression, ConvNets, GANs, RNNs, NLP, and more with TensorFlow 2 and the Keras API, 2nd Edition. Packt Publishing, 2019.

[45] https://www.worldometers.info/coronavirus/

[46] Ezz El-Din Hemdan1 , Marwa A. Shouman1 , and Mohamed Esmail Karar ," COVIDX-Net : A Framework of Deep Learning Classifiers to Diagnose COVID-19 in X-Ray Images" arXiv preprint arXiv:2003.11055.

[47] Gamal M. I.Selim Dr Hatem Khater, A. A. F. (2020). A Composite Hybrid Feature Selection Learning-Based Optimization of Genetic Algorithm For Breast Cancer Detection. 2nd International Conference on Advanced Research in Applied Science and Engineering , Which Will Be Held in Oxford, UK.

[48] Gamal M. I.Selim Dr Hatem Khater, E. A. A. F. (2020). Applying Artificial Intelligence Techniques to Improve Clinical Diagnosis of Alzheimer's Disease. The 9th International Conference on Research in Science and Technology (RSTCONF), 20-22 March 2020 in Berlin, Germany .

[49] Gamal M. I.Selim Dr Hatem Khater, E. A. A. F. (2020). A Novel Approach of CT Images Feature Analysis and Prediction to Screen for Corona Virus Disease (COVID-19). (International Journal of Scientific and Engineering Research (IJSER) - (ISSN 2229-5518, 11(3), 9.

[50] Gamal M. I.Selim Dr Hatem Khater, E. A. A. F. (2020). Applying Artificial Intelligence Techniques for Prediction of Neurodegenerative Disorders: A Comparative Case-Study on Clinical Tests and Neuroimaging Tests with Alzheimer's Disease. 2nd International Conference on Advanced Research in Applied Science and Engineering , Which Will Be Held in Oxford, UK.